Original Paper

Computational Flow Dynamics Study in Severe Carotid Bulb Stenosis with Ulceration

Tack Sun Oh, MD[1], Young Bae Ko, MS[3], Sung-Tae Park, MD[4], Kyunghwan Yoon, PhD[3], Sang-Wook Lee, PhD[5], Jee Won Park, MD[1], Jong Lim Kim, MD[1], Bohyun Kim, MD[1], Sang-Ok Park, MD[1], Jong Sung Kim, MD[2], Dae Chul Suh, MD, PhD[1]

Purpose: Computational fluid dynamics (CFD) applications for atherosclerotic carotid stenosis have not been widely used due to limited resolution in the severely stenotic lumen as well as small flow dimension in the stenotic channel.

Materials and Methods: CT data in DICOM format was transformed into 3 dimensional (3D) CFD model of carotid bifurcation. For computational analysis of blood flow in stenosis, commercial finite element software (ADINA Ver. 8.5) was used. The blood flow was assumed to be laminar, viscous, Newtonian, and incompressible. The distribution of wall shear stress (WSS), peak velocity and pressure across the average systolic and diastolic blood pressures permitted construction of a contour map of the velocity in each cardiac cycle.

Results: Computer simulation of WSS, flow velocity and wall pressure could be demonstrated three dimensionally according to flow vs. time dimension. Such flow model was correlated with angiographic finding related to maximum degree of stenosis associated with ulceration. Combination of WSS map and catheter angiogram indicated that the highest WSS corresponded to the most severely stenotic segment at systolic phase, whereas ulceration, which is the weakest point of the plaque, appeared at the downstream side of the carotid bulb stenosis.

Conclusion: Our preliminary study revealed that 3D CFD analysis in carotid stenosis was feasible from CT angiography source image and could reveal WSS, flow velocity and wall pressure in the severe carotid bulb stenosis with ulceration. Further CFD analysis is warranted to apply such hemodynamic information to the atherosclerotic lesion in the more practical way.

Key Words : Carotid arteries; Hemodynamic; Stenosis, CTA, ulceration; Wall shear stress

[1]Departments of Radiology and Research Institute of Radiology, [2]Department of Neurology, University of Ulsan, College of Medicine, Asan Medical Center; [3]Department of Mechanical Engreering, Dankook University; [4]Department of Radiology, Soonchunhyang University Hospital; [5]School of Mechanical and Automotive Engineering University of Ulsan, Seoul, Korea

Received June 29, 2010;
accepted after revision August 2, 2010.

Correspondence to: Dae Chul Suh, MD, Department of Radiology, University of Ulsan, College of Medicine, Asan Medical Center, 86 Asanbyeongwon-gil, Songpa-gu, Seoul 138-736, Korea.
Tel. 82-2-3010-4366 Fax. 82-2-476-0090 E-mail: dcsuh@amc.seoul.kr

Neurointervention 2010;5:97-102

Extracranial carotid artery atherosclerosis and subsequent ischemic strokes remain leading causes of mortality and morbidity in the western countries. Moreover, their prevalence rates are rapidly increasing even in Asian countries with westernized diet and lifestyle (1). The observation that preferential sites of atherosclerotic plaques are curved vessel, carotid bulb and arterial bifurcation has proposed the seeming correlation between hemodynamic forces and arterial disease, irrespective of systemic risk factors (2, 3). The role of hemodynamic environment in the regulation of cellular biology in normal artery, which accounts for the development and progression of atherosclerosis, has been given intense interest of research and also contributed to the development of neurointervention (4−16).

Analysis of hemodynamic parameters such as WSS magnitude and its temporal and spatial variations directly from medical imaging has been made with an implicit assumption of uniform or parabolic velocity profile. With the advancement of computer resources, computational fluid dynamics (CFD), which is the computer-aided simulation of complex flow phenomena, has emerged in the past decade as a powerful tool for studying the detailed hemodynamics of both normal and diseased vessels.

Recently, with high resolution medical imaging including X-ray angiography, computer tomography (CT), ultrasound and various magnetic resonance imaging techniques, it became possible to simulate physiologically and anatomically realistic blood flow in subject-specific manner. Although fully automated image processing tool for segmentation and reconstruction of 3-D vascular geometry from medical images is still not available, some studies demonstrated robust and objective image processing techniques with vascular geometric analysis feature.

Stenosed blood vessel creates significantly different hemodynamic environment compared to that of a normal vessel, such as transition to turbulence combined by high temporal and spatial variation of wall shear stress (WSS) which is associated with the endothelial cell damage and platelet activation. To illuminate the complex blood flow characteristics in post-stenotic regions, a variety of experimental and numerical studies have been carried out. Laser Doppler anemometry (LDA) measurements on idealized models with high degree constriction demonstrated transitional turbulent flow in post-stenotic region with intense flow disturbance (17−19). Computational simulations of pulsatile flow in stenosed tube were also conducted to explore feasibility of application of various turbulent models (20−22). However, most of these studies relied on idealized geometry and flow rates. Recently, CFD studies using patient-specific carotid models with severe stenosis presented complex flow pattern with increasing stenosis degree and emphasized the importance of using subject-specific geometries (23).

In this paper, we describe the procedure for CFD simulation of subject-specific blood flow based on CT angiography (CTA) source images and complex flow pattern in carotid bifurcation with severe stenosis. Better understanding of the hemodynamic characteristics in the stenosed carotid artery with in vivo patient-specific boundary condition will be significantly helpful in diagnosis of disease and surgical planning.

MATERIALS AND METHODS

CFD simulation of blood flow in subject-specific carotid bifurcation is usually composed of the following three phases. First, a series of high resolution 2-D slice-based medical images of carotid bifurcation in the length of interest, usually in the direction of vessel axes, which allows clearer definition of vessel lumen when acquired from CTA source images. Then outlines of vessel lumen are extracted based on pixel intensity level by various algorithms such as region growing method or level set method, and then 3-D surface is reconstructed by stacking and interpolating those segmented contours. To remove often appearing pixelization caused by low image resolution and assure appropriate smoothness of vessel lumen, surface smoothing procedure is conducted to a certain level.

In the 2nd phase, the lumen geometry obtained above should be decomposed to finite computational elements where the solutions are defined. The element size and quality should be rigorously determined to properly resolve the complex flow characteristic scale. Finer elements generally improve the accuracy of solution in complex flow regions. However, a nontrivial balance must be struck between solution accuracy and the number of element since the computational cost significantly increases with the number of elements used. The 3-D Navier-Stokes equations, which is the partial differential equations governing fluid flow phenomena, are solved numerically by discretization of various numerical schemes such as finite element method and finite volume method. The information for material properties such as blood viscosity and boundary conditions is applied as input conditions.

For the last phase, hemodynamic factors of interest,

including WSS, pressure distribution with its temporal and spatial gradient, which seems to be involved in biological responses, are computed.

Patient- specific model

Transverse contiguous 220 CTA source images of carotid bifurcation in a patient (male, 58 years) with severe stenosis were obtained using a CT imaging scanner (SOMATOM Definition, Siemens, Germany). Imaging parameters include: 1.0 mm slice thickness, 220×220 mm^2 field of view, 512×512 in-plane resolution. The calculated pixel size was 0.4297×0.4297 mm. Lumen outline for common carotid artery (CCA), internal carotid artery (ICA), external carotid artery (ECA), superior thyroid artery were extracted and reconstructed into 3-D volume. The degree of stenosis, measured by North America Symptomatic Carotid Endarterectomy Trial (NASCET) criterion which is determined by diameter ratio between distal ICA and stenosis, was more than 70%.

Flow rates

The velocity and flow rate of the internal carotid artery were obtained from gated phase contrast angiography (PCA) in a male who did not have any intracranial vascular disease. The parameters for the gated PCA synchronized to the heart cycle were: fast field echo sequence (FEE), repetition time (TR)/echo time (TE) =11/69 ms, flip angle = 15°, field of view (FOV) = 150×150 mm, matrix size = 340×312, sensitivity encoding (SENSE) factor = 3, and number of excitations (NEX) = 2. We measured the velocity (cm/s) or flow rate (mL/s) using the Quantitative-flow software, Viewforum version R 5.1 (Philips Medical Systems, Best, The Netherlands). The local Reynolds numbers in the ICA stenosis increase 355 and 1217 for the mean and peak flow rates, respectively.

Computational Fluid Dynamics

Tetrahedral elements with nominally uniform size were generated using commercially available mesh generation software, HyperMesh (Altair Engineering Inc., Auckland, New Zealand). For the computational

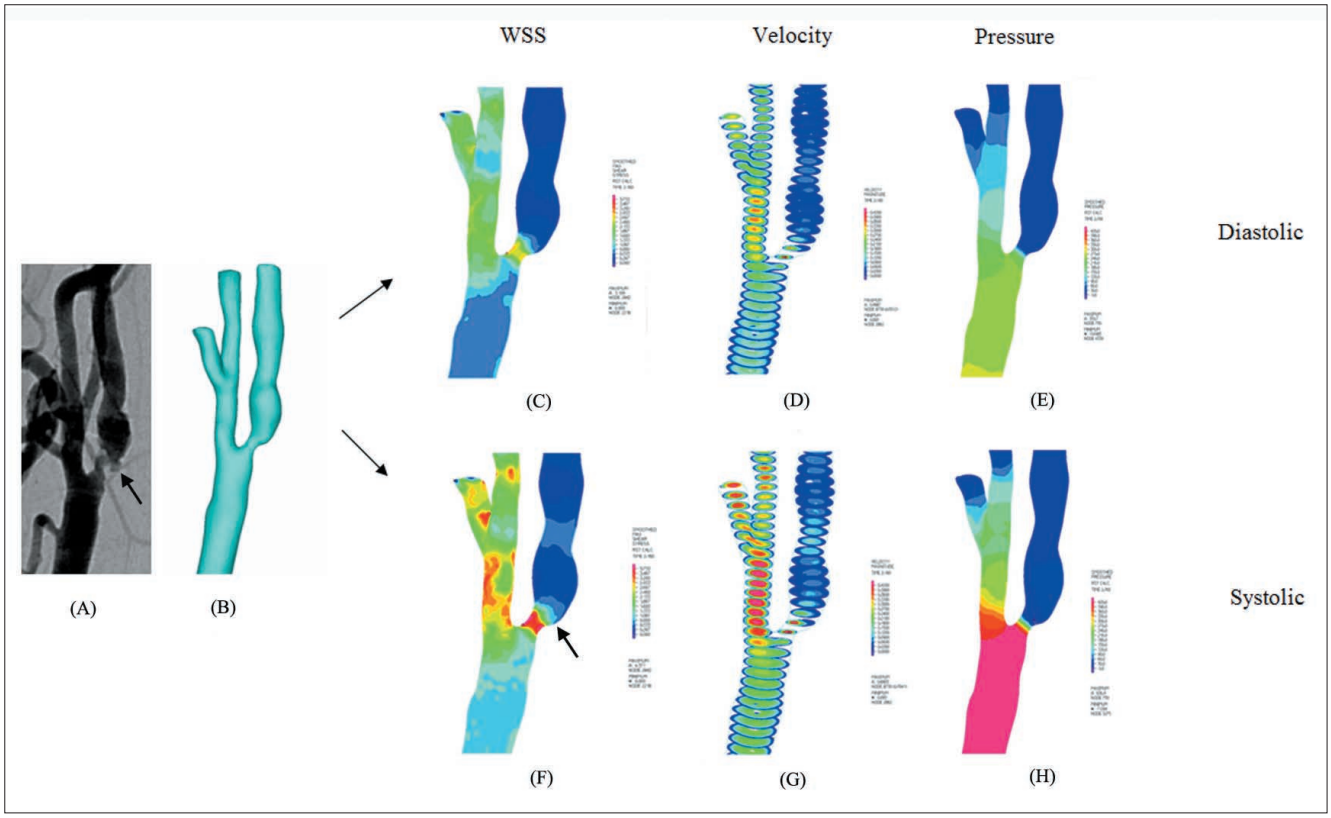

Fig. 1. A, B. Angiogram and 3-D reconstructed volume model of stenosed carotid bifurcation in 60-year-old male patient presented with the left arm weakness due to focal infacts in the left MCA borderzone area.
C-H. The distribution of WSS, peak velocity and pressure across the average diastolic and systolic blood pressures permitted construction of a contour map of the velocity in each cardiac cycle. There were high wall shear stress, peak systolic velocity and pressure gradient in systolic phase. Note an ulceration (arrow) in the carotid plaque on angiogram (**A**) which corresponds to the downstream (arrow) of the wall shear stress in (**F**).

analysis of blood flow within a stenosed carotid bifurcation, the 3-D incompressible Navier-Stokes equations were solved by a finite element based commercial CFD solver, ADINA Ver. 8.5 (ADINA R & D, Inc., Watertown, MA, U.S.A.).

Blood was assumed as Newtonian fluid and vessel wall was considered rigid. The effect of non-Newtonian characteristics of blood in the flow simulation of carotid bifurcation was shown to be only minor (24). Our simulations were performed with the following material constants: blood density, 1100 kg/m^3; and blood dynamic viscosity, 4.0 mPa · s. To achieve truly patient-specific modeling, the uniform velocity profile based on in vivo pulsatile velocity measurement was imposed at the CCA inlet. Flow division between ICA and ECA was left to be naturally determined by resistance of vessel conduit considered in the computation since the flow rates at the ICA and ECA were not available. The unsteady flow was computed for three cardiac cycles and only the results from the third cycle were considered for the analysis to ensure the independence of the initial transient solutions.

RESULTS

The distribution of WSS, peak velocity and pressure across the average systolic and diastolic blood pressures permitted construction of a contour map of the velocity in each cardiac cycle (Fig. 1). The average velocities of the carotid bifurcation in the systolic and diastolic phases were 0.73 m/s and 0.52 m/s, respectively. The WSS obtained during the three phases of one cardiac cycle revealed that the highest WSS (Fig. 1F), the highest peak systolic velocity (Fig. 1G) and maximum pressure gradient (Fig. 1 H) was present during the peak systolic phase. Combination of the WSS map and cerebral catheter angiogram indicated that the highest WSS corresponded to the most severely stenotic segment at systolic phase, whereas ulceration, which is the weakest point of the plaque, appeared at the downstream side of the carotid bulb stenosis (arrow in Fig. 1A, F). The maximum WSS of the stenotic portion of the vessel during the systolic and diastolic phases were 4.37 and 3.11 Pa, respectively.

DISCUSSION

We demonstrated that CFD analysis of severed carotid bulb stenosis with plaque was feasible with CTA source images and could be correlated with high WSS in the stenotic segment of atherosclerotic plaque and also with cerebral catheter angiogram. High WSS, increased peak velocity and pressure gradient were demonstrated at systolic rather than diastolic phase. When the high WSS area at the stenotic portion was correlated with angiogram, ulceration on angiogram was found to lie in the point beyond the maximum stenosis of the plaque, that is, the ulceration in the severe atherosclerotic plaque demonstrated on cerebral angiogram appeared at the downstream side of the carotid bulb stenosis.

Although high WSS was related to ulcerative plaque in our study, our CFD finding was opposite to Groen et al's observation which revealed the weakest location appeared at the upstream of the highest WSS region of the plaque (25). This agrees with observations that plaque-destabilizing components, including macrophages and matrix metalloproteinase-9, are highest in concentration at the upstream of the (high WSS) region of the plaque (26−28). The mechanism of stroke in our study patient with severe stenosis due to ulcerative plaque may have been related to plaque rupture associated an unstable plaque (27, 28). The earliest pathological studies described the occurrence of atherosclerosis near the branch ostia, bifurcations, and bends, suggesting flow dynamics play an important role in its induction. Because laminar flow is disturbed at carotid bifurcation regions, atherosclerotic plaque accumulation typically occurs on the outer wall of the proximal segment of the sinus of the internal carotid artery, which shows the lowest WSS. The intimal thickness is the least on the flow divider side at the junction of the internal and external carotid arteries where wall stress is the highest (29). However, Park et al. suggested that apical lesion of carotid bulb was more common among Koreans and might be related to high WSS (30, 31). Therefore further CFD study can be useful in understanding plaque development as well as stroke mechanism.

In the study of carotid endarterectomy specimens from symptomatic high-grade stenosis lesions and asymptomatic autopsy specimens without high-grade carotid artery stenosis, Bassiouny et al. (32) showed that high-grade carotid stenotic plaques were associated with significantly higher incidence of ulceration (53%), thrombosis (49%), and lumen irregularity (78%) compared with nonstenotic asymptomatic plaques (6, 0, and 17%, respectively; P _ 0.01). This finding can be associated with CFD as demonstrated in our limited study as well as other reports and may further elucidate different pathophysiological mechanisms account for stenosis of extracranial carotid

and intracranial arteries.

Our preliminary study revealed that 3 dimensional CFD analysis in carotid stenosis was feasible from CTA source image data and could reveal WSS, flow velocity and wall pressure in the severe carotid bulb stenosis with ulceration. Further CFD analysis is warranted to apply such hemodynamic information to the atherosclerotic lesion in the more practical way.

Acknowledgements and Funding

This study was supported by a grant from the Korea Healthcare Technology R&D Project, Ministry of Health & Welfare, Republic of Korea. (A080201)

References

1. Malek AM, Alper SL, Izumo S. Hemodynamic shear stress and its role in atherosclerosis. *JAMA* 1999;282:2035-2042
2. Caro CG, Fitz-Gerald JM, Schroter RC. Arterial wall shear and distribution of early atheroma in man. *Nature* 1969;223:1159-1160
3. Wootton DM, Ku DN. Fluid mechanics of vascular systems, diseases, and thrombosis. *Annu Rev Biomed Eng* 1999;1:299-329
4. Choi JW, Kim JK, Choi BS, Lim HK, Kim SJ, Kim JS, et al. Angiographic pattern of symptomatic severe M1 stenosis: comparison with presenting symptoms, infarct patterns, perfusion status, and outcome after recanalization. *Cerebrovasc Dis* 2010; 29:297-303
5. Suh DC, Kim EH. The therapeutic time window related to the presenting symptom pattern, that is, stable versus unstable patients, can affect the adverse event rate of intracranial stenting. *Stroke* 2009;40:e588-589; author reply e590
6. Liu S, Jung JH, Kwon HJ, Kim SM, Suh DC. Landmark-Wire Technique of Symptomatic Subclavian Artery Occlusion. *Interv Neuroradiol* 2009;15:401-405
7. Kim HJ, Choi BS, Choi JW, Kim SJ, Lee HY, Suh DC. Stent implantation of multichanneled pseudoocclusion of the internal carotid artery. *J Vasc Interv Radiol* 2009;20:391-395
8. Choi JW, Kim JK, Choi BS, Kim JH, Hwang HJ, Kim JS, et al. Adjuvant revascularization of intracranial artery occlusion with angioplasty and/or stenting. *Neuroradiology* 2009;51:33-43
9. Suh DC, Kim JK, Choi JW, Choi BS, Pyun HW, Choi YJ, et al. Intracranial stenting of severe symptomatic intracranial stenosis: results of 100 consecutive patients. *AJNR Am J Neuroradiol* 2008;29:781-785
10. Suh DC, Kim JK, Choi CG, Kim SJ, Pyun HW, Ahn C, et al. Prognostic factors for neurologic outcome after endovascular revascularization of acute symptomatic occlusion of the internal carotid artery. *AJNR Am J Neuroradiol* 2007;28:1167-1171
11. Pyun HW, Suh DC, Kim JK, Kim JS, Choi YJ, Kim MH, et al. Concomitant multiple revascularizations in supra-aortic arteries: short-term results in 50 patients. *AJNR Am J Neuroradiol* 2007;28:1895-1901
12. Xu GF, Suh DC, Choi CG, Kim JK, Kim W, Kim SJ, et al. Aspiration thrombectomy of acute complete carotid bulb occlusion. *J Vasc Interv Radiol* 2005;16:539-542
13. Suh DC, Lee JH, Kim SJ, Chung SJ, Choi CG, Kim HJ, et al. New concept in cavernous sinus dural arteriovenous fistula: correlation with presenting symptom and venous drainage patterns. *Stroke* 2005;36:1134-1139
14. Suh DC, Kim SJ, Lee DH, Kim W, Choi CG, Lee JH, et al. Outcome of endovascular treatment in symptomatic intracranial vascular stenosis. *Korean J Radiol* 2005;6:1-7
15. Suh DC, Lee SH, Kim KR, Park ST, Lim SM, Kim SJ, et al. Pattern of atherosclerotic carotid stenosis in Korean patients with stroke: different involvement of intracranial versus extracranial vessels. *AJNR Am J Neuroradiol* 2003;24:239-244
16. Suh DC, Sung KB, Cho YS, Choi CG, Lee HK, Lee JH, et al. Transluminal angioplasty for middle cerebral artery stenosis in patients with acute ischemic stroke. *AJNR Am J Neuroradiol* 1999;20:553-558
17. Ahmed SA, Giddens DP. Pulsatile poststenotic flow studies with laser Doppler anemometry. *J Biomech* 1984;17:695-705
18. Cassanova RA, Giddens DP. Disorder distal to modeled stenoses in steady and pulsatile flow. *J Biomech* 1978;11:441-453
19. Lieber BB, Giddens DP. Post-stenotic core flow behavior in pulsatile flow and its effects on wall shear stress. *J Biomech* 1990;23:597-605
20. Ryval J, Straatman AG, Steinman DA. Two-equation turbulence modeling of pulsatile flow in a stenosed tube. *J Biomech Eng* 2004;126:625-635
21. Stroud JS, Berger SA, Saloner D. Numerical analysis of flow through a severely stenotic carotid artery bifurcation. *J Biomech Eng* 2002;124:9-20
22. Varghese SS, Frankel SH. Numerical modeling of pulsatile turbulent flow in stenotic vessels. *J Biomech Eng* 2003;125:445-460
23. Birchall D, Zaman A, Hacker J, Davies G, Mendelow D. Analysis of haemodynamic disturbance in the atherosclerotic carotid artery using computational fluid dynamics. *Eur Radiol* 2006;16:1074-1083
24. Lee SW, Steinman DA. On the relative importance of rheology for image-based CFD models of the carotid bifurcation. *J Biomech Eng* 2007;129:273-278
25. Groen HC, Gijsen FJ, van der Lugt A, Ferguson MS, Hatsukami TS, van der Steen AF, et al. Plaque rupture in the carotid artery is localized at the high shear stress region: a case report. *Stroke* 2007;38:2379-2381
26. Saam T, Ferguson MS, Yarnykh VL, Takaya N, Xu D, Polissar NL, et al. Quantitative evaluation of carotid plaque composition by in vivo MRI. *Arterioscler Thromb Vasc Biol* 2005;25:234-239
27. Virmani R, Kolodgie FD, Burke AP, Farb A, Schwartz SM. Lessons from sudden coronary death: a comprehensive morphological classification scheme for atherosclerotic lesions. *Arterioscler Thromb Vasc Biol* 2000;20:1262-1275
28. Virmani R, Ladich ER, Burke AP, Kolodgie FD. Histopathology of carotid atherosclerotic disease. *Neurosurgery* 2006;59:S219-227; discussion S213-213
29. Glagov S, Zarins C, Giddens DP, Ku DN. Hemodynamics and atherosclerosis. Insights and perspectives gained from studies of human arteries. *Arch Pathol Lab Med* 1988;112:1018-1031
30. Park ST, Kim JK, Yoon KH, Park SO, Park SW, Kim JS, et al. Atherosclerotic carotid stenoses of apical versus body lesions in high-risk carotid stenting patients. *AJNR Am J Neuroradiol* 2010;31:1106-1112
31. Liu S, Jung JH, Kim SM, Lim HK, Kwon HJ, Kim JK, et al.

Simultaneous bilateral carotid stenting in high-risk patients. *AJNR Am J Neuroradiol* 2010;31:1113-1117
32. Bassiouny HS, Davis H, Massawa N, Gewertz BL, Glagov S, Zarins CK. Critical carotid stenoses: morphologic and chemical similarity between symptomatic and asymptomatic plaques. *J Vasc Surg* 1989;9:202-212

신경중재치료의학 2010;5:97-102

궤양을 동반한 심한 목동맥구부 협착에서의 전산유체역학 연구

오탁선[1] · 고영배[3] · 박성태[4] · 윤경환[3] · 이상욱[5] · 박지원[1] · 김종림[1] · 김보현[1] · 박상옥[1] · 김종성[2] · 서대철[1]

[1]울산대학교 의과대학 서울아산병원 영상의학과
[2]울산대학교 의과대학 서울아산병원 신경과
[3]단국대학교 기계공학과
[4]순천향대학교병원 영상의학과
[5]울산대학교 기계자동차공학부

목적: 전산유체역학 연구는 동맥류에서의 혈류분석에 주로 이용되어 왔으나 협착부의 좁은 내강과 적은 혈류량으로 인한 낮은 해상도 때문에 죽상경화성 목동맥 협착에서는 좀처럼 적용하기 어려웠다.

대상 및 방법: DICOM 형식의 CT자료를 변환하여 목동맥 분기점의 3차원 전산유체역학 모형을 구성한 후 상용유한요소 소프트웨어(ADINA Ver. 8.5)를 이용하여 협착부에서의 혈류에 대한 전산유체역학 분석을 시행하였다. 혈류는 층류, 점성, 뉴턴, 비압축성 유체로 가정하하였다. 평균 수축기혈압과 이완기혈압 사이의 벽면전단응력, 최대속도, 벽면압 분포를 이용하여 매 심장주기에서의 속도등고선지도를 완성하였다.

결과: 벽면전단응력, 혈류속도, 벽면압의 전산화 모의실험을 혈류-시간에 따라 삼차원적으로 표현하였다. 재구성된 혈류모형은 최대 협착부에서의 혈관조영술 소견과 잘 일치하였다. 벽면전단응력지도와 혈관조영술 결과를 종합하였을 때 혈관조영술에서의 최대협착부와 최고벽면전단응력부가 일치하였으며, 죽상판의 최고취약부인 궤양은 협착을 지난 부위의 낮은 벽면전단응혈류에서 나타났다.

결론: 본 예비연구는 CTA의 영상자료를 이용한 삼차원 전산유체역학 분석이 가능함을 밝혔고, 궤양을 동반한 심한 목동맥구부 협착에서의 벽면전단응력, 혈류속도, 벽면압을 규명하였다. 전산유체역학 분석은 혈역학 정보를 죽상경확성 병변에 실용적으로 적용함에 있어 중요한 역할을 할 것으로 기대된다.

Key Words : Carotid arteries; Hemodynamic; Stenosis, CTA, ulceration; Wall shear stress